

Article

A Single-Variable Zigzag Approach to Model Imperfect Interfaces in Layered Beams

Iliaria Monetto *  and Roberta Massabò 

Department of Civil, Chemical and Environmental Engineering, University of Genoa, 16145 Genova, Italy

* Correspondence: ilaria.monetto@unige.it

Abstract: The flexibility of the bonds between the adjacent layers of multi-layered systems and their degradation or the presence of delaminations strongly affect mechanical response and final collapse. The formulation of accurate and efficient models able to capture the complex local distributions of stresses and displacements, which arise due to the layered structure and imperfect bonding, is of great importance for the design and verification of the systems. In this paper a novel and effective “single-variable zigzag” theory is formulated to analyze beams with homogeneous layers made of the same material and imperfect interfaces, which allow sliding between the layers. The primal variable is a fictitious bending displacement, which is derived in order to define all other kinematic and static quantities in terms of it. The “zigzag” technique describes multilayer systems with imperfect interfaces as equivalent single-layers, so that the problem is governed by equations similar to those of the classical theories for homogeneous beams; the “single-variable” formulation facilitates the implementation into numerical schemes and eliminates well-known numerical problems. Explicit solutions are straightforwardly derived for simply supported beams subjected to uniform and sinusoidal transverse loads. The results for some exemplary structural elements confirm the accuracy and efficiency of the approach. The study is preliminary to the single-variable reformulation and numerical implementation of the zigzag models for laminates with elastic mismatch between the layers.

Keywords: layered beams; zigzag theories; single-variable formulation; interfaces; delaminations



Citation: Monetto, I.; Massabò, R. A Single-Variable Zigzag Approach to Model Imperfect Interfaces in Layered Beams. *Coatings* **2023**, *13*, 445. <https://doi.org/10.3390/coatings13020445>

Academic Editors: Frédéric C. Lebon, Raffaella Rizzoni and Maria Letizia Raffa

Received: 18 December 2022

Revised: 7 February 2023

Accepted: 13 February 2023

Published: 15 February 2023



Copyright: © 2023 by the authors. Licensee MDPI, Basel, Switzerland. This article is an open access article distributed under the terms and conditions of the Creative Commons Attribution (CC BY) license (<https://creativecommons.org/licenses/by/4.0/>).

1. Introduction

Layered systems, laminated and sandwich composites are used in various applications requiring high strength/stiffness to weight ratios, such as in structures for sustainable marine, aerial and land mobility. They also find application in other classical and emerging fields, from civil engineering to electronics. The layered architecture and the presence of deformable or damaged interfaces, and delaminations, have important effects on the local stress and displacement fields which cannot be predicted using classical beam/plate theories for homogeneous structures or equivalent single layer theories [1–4]. The analysis of such systems is not straightforward but of fundamental importance to control excessive reductions of global stiffness or ultimate loads and failure by delamination [2,3]. They are typically studied using discrete-layer structural theories [4,5], or through homogenized models, such as the zigzag model used in this work [6–13].

Single-variable approaches to the analysis of structural problems characterized by more than one variable are more convenient than standard approaches since they facilitate the derivation of analytical solutions and allow us to overcome problems exhibited by the numerical solution schemes [14,15]. In numerical finite element methods, for instance, the discretization of the kinematic unknowns is usually performed using the same shape functions, independently of the physical dimensions of the unknowns (displacements and/or rotations) and of the consistency of the related discrete spaces. As a result, the problem of shear locking may arise [16].

In single-variable approaches the system of coupled differential equations, that commonly governs any mechanical problem, is reduced to a single equation in one unknown variable, called primal variable. The primal variable is chosen among the effective variables or as a new fictitious variable, which is defined ad hoc so that all other variables can be explicitly expressed in terms of the primal one. It is evident that such approaches exclude a priori locking problems [17], because only one variable needs discretization.

Efficient single-variable approaches were recently proposed in [18,19] for the solution of homogeneous Timoshenko beams (two variables in the classical approach), where different choices for the primal variable were considered and discussed. These works inspired the derivation of novel single-variable formulations for the analysis of laminated beams, which were presented in [20,21] for perfectly bonded interfaces in the framework of both classical first-order shear deformation laminate and zigzag theories (three variables in the classical approach). The attention was focused on the effects of the elastic mismatch between the layers of composite beams, which is responsible for complex zigzag distributions of stresses and displacements in the thickness direction, and on the development and implementation of isogeometric collocation schemes (see, e.g., [18,19,22]), useful to solve numerically more complex problems. Some promising preliminary results were obtained and confirmed the validity of the method and the feasibility of its extension to the analysis of multi-layered systems with imperfect interfaces.

In this paper we propose the extension of the single-variable approach in [20,21] to the zigzag model in [23] for beams with homogeneous layers and imperfect interfaces. The model in [23] was built on the multiscale model originally formulated in [24] for laminated plates and later applied to the solution of a wide class of problems: plane-strain problems [25]; propagation of plane-strain harmonic waves [26]; brittle delamination fracture under mode II dominant conditions [27,28]. The limitation to laminates consisting of layers made of the same material excludes the influence of the elastic mismatch between the layers and allows us to highlight and discuss the capabilities of the model, which is able to accurately describe, with just one variable, the effects of the relative displacements occurring at partially bonded layer interfaces. The goal of the paper is then to assess the performance and accuracy of the single-variable approach when applied to a zigzag theory including imperfect interfaces. This is preliminary to the future extension of the approach to the analysis of laminates with elastic mismatch between the layers and to the numerical implementation.

In Section 2 we first review the original zigzag theory and then show how the governing equations can be decoupled and reduced to a single equation in only one variable. The equation coefficients evaluated for beams consisting of two and three layers with equal thicknesses are listed in Appendix A, whereas the explicit solution for the single-variable equation is reported in Appendix B for the two loading conditions of uniform and sinusoidal transverse loads. In Section 3 our formulation is verified through the analysis of the local response of two- and three-layered simply supported beams. The effects of partially bonded interfaces are widely discussed. The conclusions are presented in Section 4.

2. Materials and Methods

The layered beam considered in the present model is shown in Figure 1. A system of Cartesian coordinates x_1, x_2, x_3 is introduced with the axis x_3 normal to the reference surface of the beam, which can be chosen arbitrarily.

The beam has thickness h and length L and consists of n layers having constant cross section and made of the same homogeneous, linearly elastic and orthotropic material, with principal material axes parallel to the geometrical axes. The layer k (with $k = 1, \dots, n$ numbered from bottom to top) has thickness $^{(k)}h$.

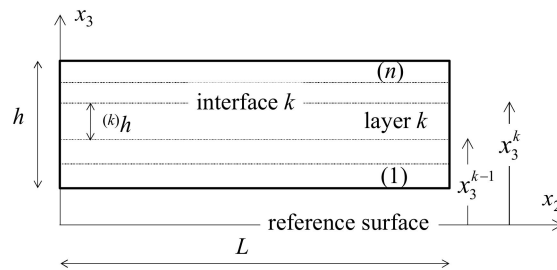


Figure 1. Layered beam geometry.

The $n - 1$ interfaces joining the layers were treated as continuous zero-thickness mathematical surfaces, where only relative sliding displacements may occur, and relative transverse displacements are not allowed. This assumption neglected the presence of transition zones between the adjacent layers, which may occur in practice, due to manufacturing processes, and require to be suitably modelled [29]. The assumption of sharp interface was adequate when the thickness of such transition zones was small compared to the layer thickness. Future extension of the single variable approach, accounting for the elastic mismatch between the adjacent layers, will allow to analyze also the effects of interlayers modelled as weak layers [30].

The sliding displacements at the interfaces were controlled by interfacial shear tractions through linear interfacial constitutive laws. The interface k (with $k = 1, \dots, n - 1$ numbered from bottom to top) has coordinate x_3^k and interfacial tangential stiffness K_S^k . For fully bonded adjacent layers $1/K_S^k \rightarrow 0$ (perfect interface), so that no relative displacement occurred. Partial bonding between the adjacent layers is characterized by $K_S^k > 0$ (imperfect interface). In this case relative sliding occurred and proportional interfacial shear tractions were transmitted across the interface. For a fully de-bonded interface $K_S^k = 0$ (delamination) and no interfacial shear tractions were transmitted across the interface.

The beam was subjected to transverse mechanical loads applied on the upper, lower and lateral bounding surfaces, so that the beam was under plane strain conditions parallel to the plane $x_2 - x_3$. Residual stresses due to manufacturing or production processes, and thermal stresses induced by thermal gradients under extreme environment conditions were not considered. However, their contributions could be straightforwardly taken into account, following the extension of the original zigzag model presented in [23].

The equilibrium problem for the layered beam is analyzed under the assumptions of:

- Small displacements, rotations and strains;
- Transverse normal stresses negligibly small compared to the other components and set equal to zero ($\sigma_{33} = 0$).

A zigzag kinematic approximation was assumed, according to which the global displacement field of standard first-order shear deformation theory, which was continuous with continuous derivatives in the thickness direction, was locally enriched in order to reproduce the zigzag patterns and the jumps at the interfaces. The enrichment functions were derived on imposing continuity conditions on the transverse shear stresses and the relationship between interfacial tractions and jumps at the interfaces. All details of the derivations can be found in [23], where a general formulation including the effects of elastic mismatch between the adjacent layers is proposed.

The local displacement field in the generic layer k was then written as follows

$$\begin{aligned} {}^{(k)}v_2(x_2, x_3) &= v_{02}(x_2) + x_3\varphi_2(x_2) + [\varphi_2(x_2) + w_{0,2}(x_2)]R_{S22}^k(x_3) , \\ {}^{(k)}v_3(x_2, x_3) &= w_0(x_2) \end{aligned} \tag{1}$$

with

$$R_{S22}^k(x_3) = \sum_{i=1}^{k-1} \frac{C_{44}}{K_S^i} \tag{2}$$

where: $^{(k)}v_i$ with $i = 2,3$ is the local displacement in the layer k along the direction x_i , whereas $^{(k)}v_1 = 0$ for the assumed plane-strain conditions; v_{02}, w_0 and φ_2 denote the global degrees of freedom, which were continuous with continuous derivatives in the thickness direction; C_{44} is the stiffness coefficient relating local shear stresses and strains for the layer material through $^{(k)}\sigma_{23} = C_{44}2^{(k)}\varepsilon_{23}$ with $2^{(k)}\varepsilon_{23} = ^{(k)}v_{2,3} + ^{(k)}v_{3,2}$. Equation (2) represents the enrichment applied to the global longitudinal displacement field (linear through the thickness) to account for the effects of the jumps at the imperfect interfaces.

The local stress field in the generic layer k was obtained from Equation (1) through 2D compatibility and constitutive equations

$$\begin{aligned} ^{(k)}\sigma_{22}(x_2, x_3) &= \bar{C}_{22} \left\{ v_{02,2}(x_2) + x_3\varphi_{2,2}(x_2) + [\varphi_{2,2}(x_2) + w_{0,22}(x_2)]R_{S22}^k(x_3) \right\}, \quad (3) \\ ^{(k)}\sigma_{23}(x_2, x_3) &= C_{44}[\varphi_2(x_2) + w_{0,2}(x_2)] \end{aligned}$$

where a comma followed by a subscript denotes derivation with respect to x_2 ; $\bar{C}_{22} = (C_{22} - C_{23}C_{32}/C_{33})$ relates local longitudinal normal stresses and strains through $^{(k)}\sigma_{22} = \bar{C}_{22}^{(k)}\varepsilon_{22}$ for the assumed plane-strain conditions, where C_{22}, C_{23}, C_{32} and C_{33} are the coefficients of the 6x6 stiffness matrix of the layer material.

The interfacial tractions at the interface k are common to the layers k and $k + 1$ and were related to the interfacial displacements by

$$^{(k)}\sigma_{23}(x_2, x_3 = x_3^k) = ^{(k+1)}\sigma_{23}(x_2, x_3 = x_3^k) = K_S^k [^{(k+1)}v_2(x_2, x_3 = x_3^k) - ^{(k)}v_2(x_2, x_3 = x_3^k)]. \quad (4)$$

The homogenized equilibrium equations governing the problem were derived using the Principle of Virtual Work and taking into account Equations (1)–(4). In terms of the global displacements, they are given by

$$\begin{aligned} A_{22}v_{02,22} + B_{22}\varphi_{2,22} + C_{22}^{0S}(\varphi_2 + w_{0,2})_{,22} &= 0 \\ (B_{22} + C_{22}^{0S})v_{02,22} + (D_{22} + C_{22}^{1S})\varphi_{2,22} + (C_{22}^{1S} + C_{22}^{S2})(\varphi_2 + w_{0,2})_{,22} - A_{44}(\varphi_2 + w_{0,2}) &= 0, \quad (5) \\ C_{22}^{0S}v_{02,222} + C_{22}^{1S}\varphi_{2,222} + C_{22}^{S2}(\varphi_2 + w_{0,2})_{,222} - A_{44}(\varphi_2 + w_{0,2})_{,2} - f_3 &= 0 \end{aligned}$$

with coefficients

$$\begin{aligned} (A_{22}, B_{22}, D_{22}) &= \sum_{k=1}^n \bar{C}_{22} \int_{x_3^{k-1}}^{x_3^k} (1, x_3, x_3^2) dx_3, \quad C_{22}^{S2} = \sum_{k=1}^n \bar{C}_{22} (R_{S22}^k)^2 ^{(k)}h, \\ (C_{22}^{0S}, C_{22}^{1S}) &= \sum_{k=1}^n \bar{C}_{22} R_{S22}^k \int_{x_3^{k-1}}^{x_3^k} (1, x_3) dx_3, \quad A_{44} = k_{44}C_{44}h + \sum_{k=1}^{n-1} \frac{(C_{44})^2}{K_S^k}, \end{aligned} \quad (6)$$

where f_3 denotes the distributed transverse global load (positive if upward). The coefficients A_{22} and D_{22} are the extensional and bending laminate stiffnesses; B_{22} is the coupling stiffness of the laminate and relates bending strain with normal force and vice-versa. Note that, for the homogeneous laminates under consideration, $B_{22} = 0$ when the reference surface $x_3 = 0$ was chosen at the mid-thickness plane; however, the membrane and bending equilibrium problems remained coupled due to the presence of the coefficient C_{22}^{0S} , which was related to the imperfect interfaces. The shear correction factor k_{44} introduced in A_{44} allowed us to improve the treatment of shear, given the limitations of the first-order shear deformation theory used to describe the global kinematics [3]. The coefficients for homogeneous laminates consisting of two and three layers having equal thickness are listed in Appendix A.

Equation (5) is a system of three coupled differential equations in the three unknowns v_{02}, w_0 and φ_2 with boundary conditions prescribed at the ends $x_2 = 0, L$ with outward normals $\mathbf{n} = \{0, \mp 1, 0\}^T$ on the kinematic and/or static energetically consistent quantities.

$$\begin{aligned} v_{02} \text{ or } N_{22}n_2 &= [A_{22}v_{02,2} + B_{22}\varphi_{2,2} + C_{22}^{0S}(\varphi_2 + w_{0,2})_{,2}]n_2 \\ w_0 \text{ or } Q_{22}n_2 &= [-C_{22}^{0S}v_{02,22} - C_{22}^{1S}\varphi_{2,22} - C_{22}^{S2}(\varphi_2 + w_{0,2})_{,22} + A_{44}(\varphi_2 + w_{0,2})]n_2 \\ \varphi_2 \text{ or } M_{22}n_2 &= [(B_{22} + C_{22}^{0S})v_{02,2} + (D_{22} + C_{22}^{1S})\varphi_{2,2} + (C_{22}^{1S} + C_{22}^{S2})(\varphi_2 + w_{0,2})_{,2}]n_2 \\ w_{0,2} \text{ or } M_{22}^{ZS}n_2 &= [C_{22}^{0S}v_{02,2} + C_{22}^{1S}\varphi_{2,2} + C_{22}^{S2}(\varphi_2 + w_{0,2})_{,2}]n_2 \end{aligned} \quad (7)$$

When the layers were perfectly bonded ($1/K_S^k \rightarrow 0$ for all $k = 1, \dots, n - 1$), all coefficients with upperscript S vanish and Equations (5)–(7) coincided with those of first-order shear deformation theory.

The system of coupled differential Equations (5)–(7) were here decoupled and a single equation in only one unknown variable was obtained. In order to do this, we followed the approach proposed in [18] and split the global transverse displacement w_0 into a bending part, w_{0b} , and a shear part, w_{0s} , which are defined as follows

$$w_0 = w_{0b} + w_{0s}, \quad \varphi_2 = -w_{0b,2}, \quad \varphi_2 + w_{0,2} = w_{0s,2}. \tag{8}$$

The bending part w_{0b} was then selected as primal variable. This special choice of a fictitious bending displacement as primal variable allowed us to express all kinematic and static variables in terms of the new primal variable and its derivatives and was shown to be particularly efficient for future implementation in numerical solution schemes.

Substituting Equation (8) into Equation (5) yielded

$$\begin{aligned} A_{22}v_{02,22} - B_{22}w_{0b,222} + C_{22}^{0S}w_{0s,222} &= 0 \\ (B_{22} + C_{22}^{0S})v_{02,22} - (D_{22} + C_{22}^{1S})w_{0b,222} + (C_{22}^{1S} + C_{22}^{S2})w_{0s,222} - A_{44}w_{0s,2} &= 0 ; \\ C_{22}^{0S}v_{02,222} - C_{22}^{1S}w_{0b,2222} + C_{22}^{S2}w_{0s,2222} - A_{44}w_{0s,22} - f_3 &= 0 \end{aligned} \tag{9}$$

whereas deriving once with respect to x_2 the first and second of Equation (9) gave

$$\begin{aligned} A_{22}v_{02,222} - B_{22}w_{0b,2222} + C_{22}^{0S}w_{0s,2222} &= 0 \\ (B_{22} + C_{22}^{0S})v_{02,222} - (D_{22} + C_{22}^{1S})w_{0b,2222} + (C_{22}^{1S} + C_{22}^{S2})w_{0s,2222} - A_{44}w_{0s,22} &= 0 \end{aligned} \tag{10}$$

Combining Equation (10) with the third of Equation (9), $v_{02,222}$ and $w_{0s,22}$ were expressed in terms of w_{0b} and its derivatives. Introducing such results into the third of Equation (9), a sixth-order differential equation in the unknown w_{0b} was finally obtained

$$w_{0b,222222} + \Omega_4 w_{0b,2222} = \Omega_3 f_3 + \Omega_2 f_{3,22}, \tag{11}$$

where

$$\begin{aligned} \Omega_4 &= A_{44}D^{-1} [A_{22}D_{22} - (B_{22})^2] \\ \Omega_3 &= A_{44}D^{-1}A_{22} \\ \Omega_2 &= D^{-1} [B_{22}C_{22}^{0S} + (C_{22}^{0S})^2 - A_{22}(C_{22}^{1S} + C_{22}^{S2})] \end{aligned} \tag{12}$$

with

$$D = (B_{22})^2 C_{22}^{S2} + (C_{22}^{0S})^2 D_{22} + A_{22} [(C_{22}^{1S})^2 - C_{22}^{S2} D_{22}] - 2B_{22}C_{22}^{0S}C_{22}^{1S}. \tag{13}$$

When w_{0b} was determined as solution of the differential Equation (11), which contained six arbitrary constants c_i with $i = 1, \dots, 6$, the global rotation φ_2 followed directly from the second of Equation (8); the global transverse displacement w_0 followed from the first of Equation (8).

$$w_0 = w_{0b} + w_{0s} \text{ with } w_{0s} = W_4 w_{0b,2222} + W_2 w_{0b,22} + W_f f_3, \tag{14}$$

where

$$\begin{aligned} W_4 &= D [B_{22}C_{22}^{0S} + (C_{22}^{0S})^2 - A_{22}(C_{22}^{1S} + C_{22}^{S2})] / [A_{22}(A_{44})^2 (A_{22}C_{22}^{1S} - B_{22}C_{22}^{0S})] \\ W_2 &= [(B_{22})^2 + B_{22}C_{22}^{0S} - A_{22}(C_{22}^{1S} + D_{22})] / (A_{22}A_{44}) \\ W_f &= [B_{22}C_{22}^{0S} + (C_{22}^{0S})^2 - A_{22}(C_{22}^{1S} + C_{22}^{S2})]^2 / [A_{22}(A_{44})^2 (B_{22}C_{22}^{0S} - A_{22}C_{22}^{1S})] \end{aligned} \tag{15}$$

The global longitudinal displacement v_{02} followed from the integration of the first of Equation (9), also using the second of Equation (14), and required the introduction of two additional arbitrary constants c_7 and c_8 , as follows

$$v_{02} = V_3 w_{0b,222} + V_1 w_{0b,2} + V_f \int f_3 dx_2 + c_7 x_2 + c_8, \tag{16}$$

with

$$\begin{aligned} V_3 &= DC_{22}^{0S} / [A_{22}A_{44}(A_{22}C_{22}^{1S} - B_{22}C_{22}^{0S})] \\ V_1 &= B_{22}/A_{22} \\ V_f &= C_{22}^{0S} [B_{22}C_{22}^{0S} + (C_{22}^{0S})^2 - A_{22}(C_{22}^{1S} + C_{22}^{S2})] / [A_{22}A_{44}(B_{22}C_{22}^{0S} - A_{22}C_{22}^{1S})] \end{aligned} \tag{17}$$

The single-variable boundary value problem governed by Equations (11)–(17) was completed by eight boundary conditions, imposed at the beam ends $x_2 = 0, L$ on the global displacements or on the force and moment resultants according to Equation (7).

It is worthwhile noting that the general solution of the sixth-order linear differential Equation (11) in the primal variable w_{0b} could be obtained quite straightforwardly and could be written in different forms depending on the constant coefficients, which can either vanish or be positive or negative for given thickness and material of the layers and stiffness of the interfaces. As an example, in Appendix B the general solution of Equation (11) was provided for laminate beams satisfying the condition $\Omega_4 < 0$, as in the case of layers having equal thickness and with a mid-thickness reference surface.

Finally, once the boundary value problem had been solved, the local response for each layer and interface was obtained straightforwardly through Equations (1)–(4), but for the transverse shear stresses, which were calculated a posteriori by satisfying local equilibrium ${}^{(k)}\sigma_{22,2} + {}^{(k)}\sigma_{23,3}^{post} = 0$. Local equilibrium also led to an equilibrium solution for the transverse normal stresses, ${}^{(k)}\sigma_{23,2} + {}^{(k)}\sigma_{33,3}^{post} = 0$.

3. Results and Discussion

This section presents the application of the single-variable formulation developed in the paper to the analysis of two classical problems shown in Figure 2. A laminated beam was simply supported at the ends and subjected to two loading conditions: a sinusoidal transverse load $f_3(x_2) = q_0 \sin(\pi x_2/L)$ (Figure 2a) and a uniform transverse load $f_3(x_2) = q_0$ (Figure 2b).

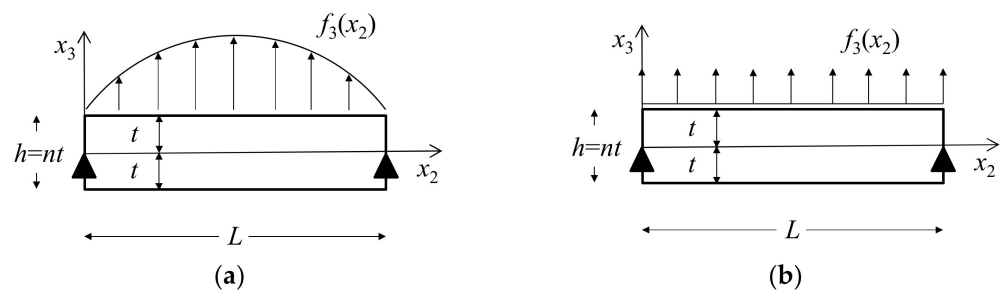


Figure 2. Simply supported beams subjected to: (a) sinusoidal and (b) uniform transverse loads.

The former problem is a classical study case, which was solved exactly within 2D elasticity for perfectly bonded interfaces by Pagano [31] and more recently for elastic interfaces in [32]. Its 1D solution according to the model presented in Section 2 was given by Equation (B1) and Equation (B2). The 1D solution of the problem in Figure 2b, according to our model, was given by Equations (B1) and (B3). For both problems the

arbitrary constants in Equation (B1) were determined by imposing the boundary conditions corresponding to simply supported ends, that is

$$\begin{aligned} w_0(x_2 = 0) = w_0(x_2 = L) = 0, \quad v_{02}(x_2 = 0) = 0, \quad N_{22}(x_2 = L) = 0, \\ M_{22}(x_2 = 0) = M_{22}(x_2 = L) = 0, \quad M_{22}^{ZS}(x_2 = 0) = M_{22}^{ZS}(x_2 = L) = 0. \end{aligned} \tag{18}$$

The beam under consideration had length $L = 5h$ and consisted of n layers of equal thickness ($t = h/n$) connected through elastic interfaces. In the applications, two- and three-layer beams ($n = 2,3$) with stacking sequences $(0^\circ/0^\circ)$ and $(0^\circ/0^\circ/0^\circ)$, respectively, were considered. Each lamina was assumed to be orthotropic with elastic constants $E_L, E_T = E_L/25, G_{LT} = E_L/50, G_{TT} = E_L/125, \nu_{LT} = \nu_{TT} = 0.25$. In all cases a mid-thickness reference surface was chosen.

All results shown in what follows have been obtained for $k_{44} = 5/6$. In Figures 3–8 the dimensionless through-the-thickness longitudinal displacement, and bending and transverse shear stresses are shown for different values of the interfacial stiffness. Pagano’s 2D-model-based exact solutions are also shown for both imperfect (red solid lines) and perfect (red dotted lines) interfaces.

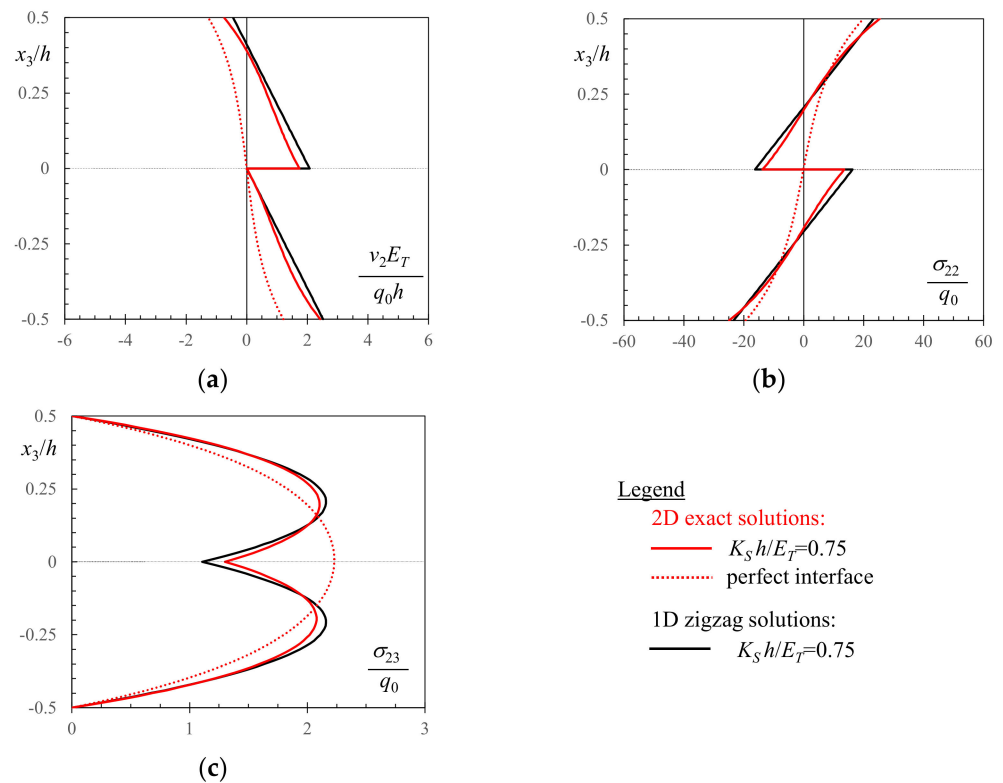


Figure 3. 2D exact and 1D zigzag solutions for simply supported two-layer beam $(0^\circ/0^\circ)$ with $L/h = 5$ subjected to sinusoidal transverse load: (a) local longitudinal displacements (at $x_2 = 0$); (b) bending stresses (at $x_2 = 0.5L$); (c) transverse shear stresses (at $x_2 = 0$) determined from local equilibrium. The red dotted lines correspond to the 2D exact solution for perfectly bonded interface.

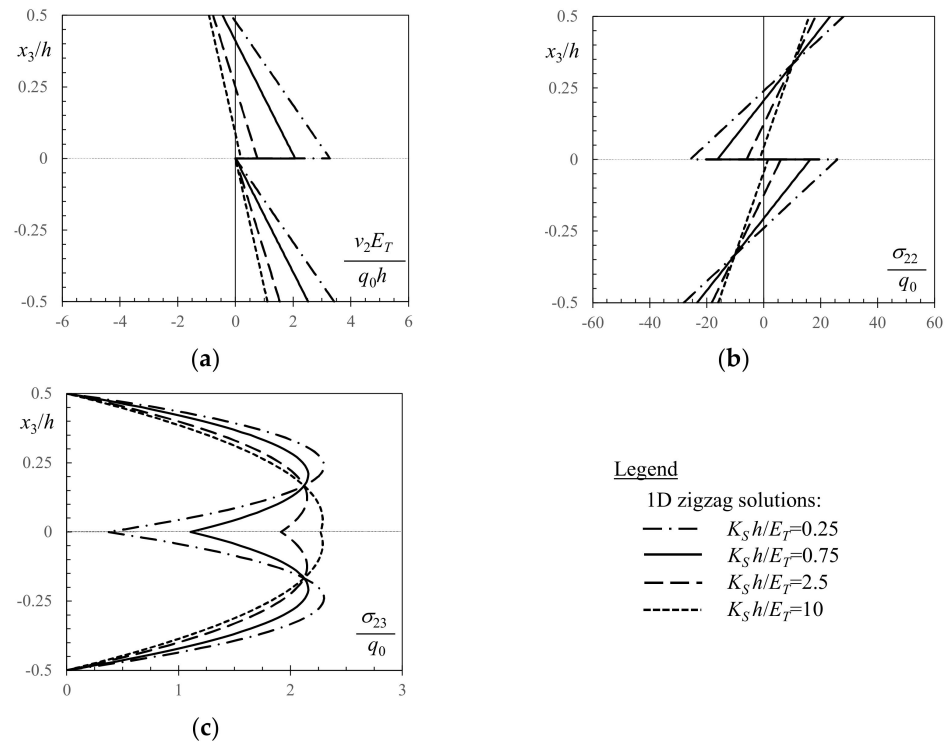


Figure 4. 1D zigzag solutions for simply supported two-layer beam ($0^\circ/0^\circ$) with $L/h = 5$ subjected to sinusoidal transverse load: (a) local longitudinal displacements (at $x_2 = 0$); (b) bending stresses (at $x_2 = 0.5L$); (c) transverse shear stresses (at $x_2 = 0$) determined from local equilibrium.

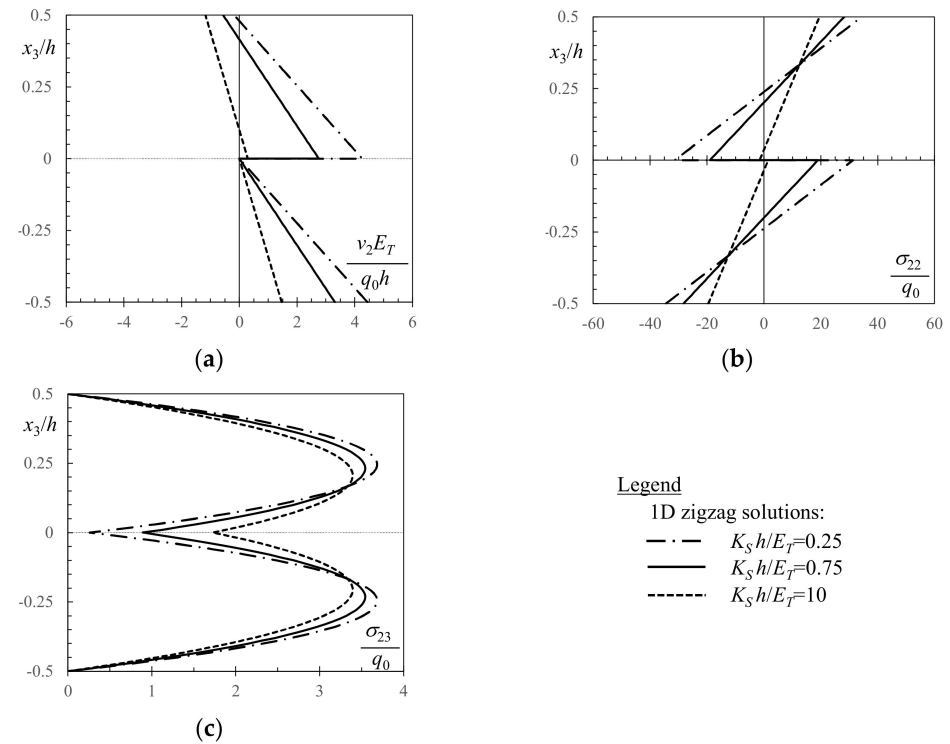


Figure 5. 1D zigzag solutions for simply supported two-layer beam ($0^\circ/0^\circ$) with $L/h = 5$ subjected to uniform transverse load: (a) local longitudinal displacements (at $x_2 = 0$); (b) bending stresses (at $x_2 = 0.5L$); (c) transverse shear stresses (at $x_2 = 0$) determined from local equilibrium.

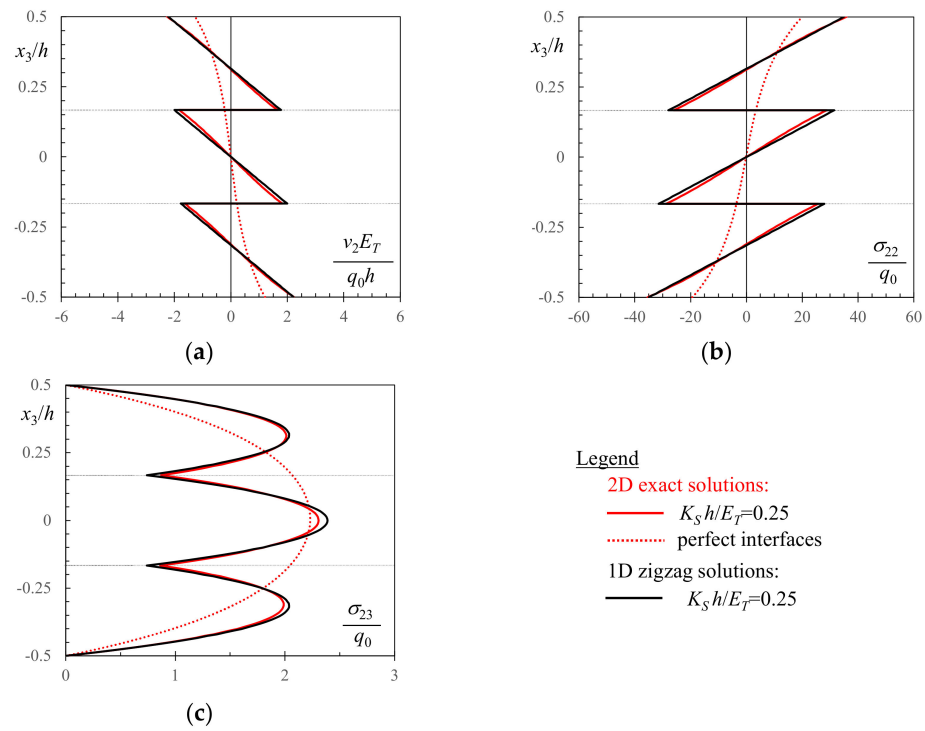


Figure 6. 2D exact and 1D zigzag solutions for simply supported three-layer beam ($0^\circ/0^\circ/0^\circ$) with $L/h = 5$ having interfaces of equal stiffness and subjected to sinusoidal transverse load: (a) local longitudinal displacements (at $x_2 = 0$); (b) bending stresses (at $x_2 = 0.5L$); (c) transverse shear stresses (at $x_2 = 0$) determined from local equilibrium. The red dotted lines correspond to the 2D exact solution for perfectly bonded interfaces.

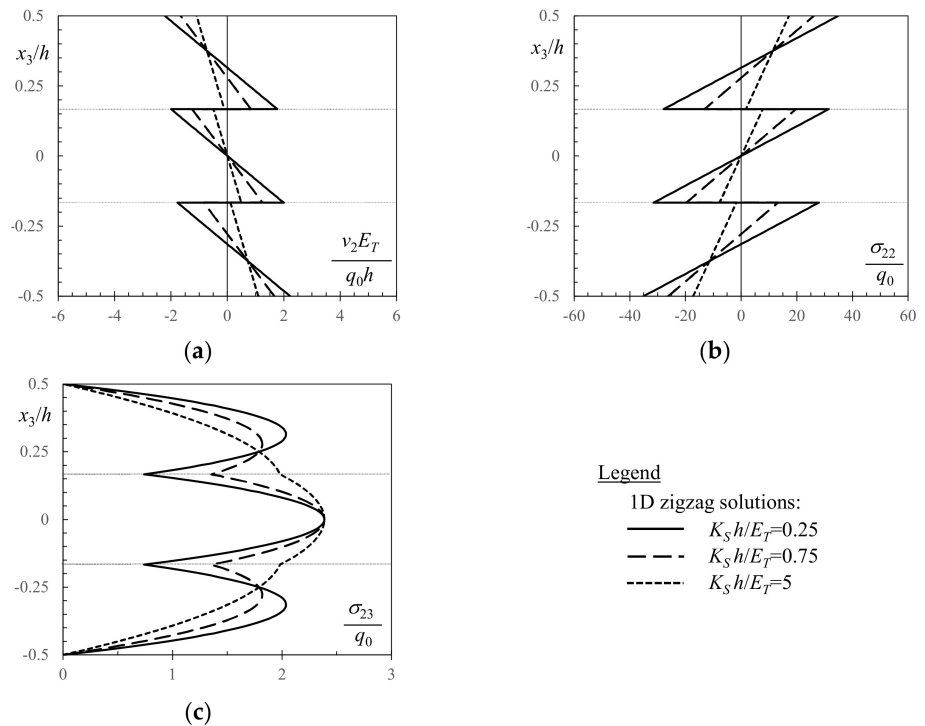


Figure 7. 1D zigzag solutions for simply supported three-layer beam ($0^\circ/0^\circ/0^\circ$) with $L/h = 5$ having interfaces of equal stiffness and subjected to sinusoidal transverse load: (a) local longitudinal displacements (at $x_2 = 0$); (b) bending stresses (at $x_2 = 0.5L$); (c) transverse shear stresses (at $x_2 = 0$) determined from local equilibrium.

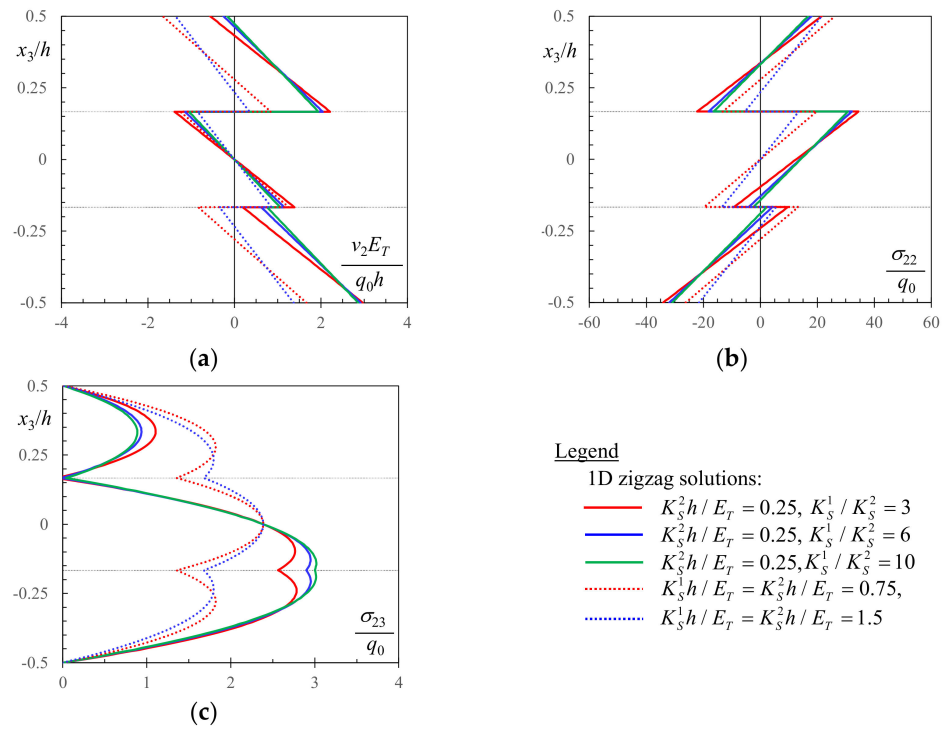


Figure 8. 1D zigzag solutions for simply supported three-layer beam ($0^\circ/0^\circ/0^\circ$) with $L/h = 5$ having interfaces of different stiffness ($K_S^2h/E_T = 0.25$) and subjected to sinusoidal transverse load: (a) local longitudinal displacements (at $x_2 = 0$); (b) bending stresses (at $x_2 = 0.5L$); (c) transverse shear stresses (at $x_2 = 0$) determined from local equilibrium. The dotted lines correspond to the solutions for both interfaces having equal stiffness $K_S^1h/E_T = K_S^2h/E_T = 0.75$ (red dotted lines) and 1.5 (blue dotted lines).

Figure 3 shows the local response for a simply supported two-layer beam with stacking sequence ($0^\circ/0^\circ$) subjected to sinusoidal transverse load (Figure 2a) and having the elastic interface of stiffness $K_S^1h/E_T = K_Sh/E_T = 0.75$. In these diagrams the 1D zigzag-kinematic-based analytical results (black solid lines) are compared with Pagano’s 2D exact solution (red solid lines). The comparison highlights the accuracy of the 1D zigzag-kinematic-based results. Slight differences in the interfacial jumps of longitudinal displacement and bending stress, as well as in the peak values of transverse shear stress, were due to the kinematic assumptions of the approximate zigzag model, which assumed the longitudinal displacement as a piece-wise linear function of the through-thickness coordinate with jumps at the interfaces. As shown in Figure 3a, the displacements of the more accurate elasticity solution were nonlinear within each layer.

Pagano’s 2D exact solution for the perfectly bonded interface is also shown (red dotted lines) in order to highlight how strongly the interfacial compliance affected the local response. Significant jumps occurred at the interfaces and the absolute values of local displacements and stresses increased.

Figure 4 shows the results for varying interfacial stiffnesses $K_S^1h/E_T = K_Sh/E_T = 0.25$ (black dash-dotted lines), 0.75 (black solid lines), 2.5 (black dashed lines) and 10 (black dotted lines). Very low interfacial stiffnesses are indicative of weak bonds between the adjacent layers. The global response tends to that of separate layers. Very high interfacial stiffnesses are indicative of strong bonds between the adjacent layers. The global response tends to that of perfectly bonded layers. From the results in Figure 4 the following conclusions can also be drawn. The more compliant the interface, the higher the local displacements and stresses in the layers. As expected, the response tends to that for a perfect interface on increasing the interfacial stiffness, and for $K_Sh/E_T = 10$ the solution nearly overlapped to that for perfectly bonded interface.

Analogous considerations can be drawn from Figure 5, where the local response for the same beam subjected to uniform transverse load (Figure 2b) is shown. The loading condition appeared to play a secondary role in comparison to that of the interfacial stiffness. A verification of the accuracy of the zigzag model for the systems in Figures 3 and 4 was presented in [24].

Figure 6 shows the local response for a simply supported three-layer beam with stacking sequence ($0^\circ/0^\circ/0^\circ$), interfaces of equal stiffness and subjected to sinusoidal transverse load. The 1D

zigzag-kinematics-based analytical results are presented for interfacial stiffness $K_S^1 h/E_T = K_S^2 h/E_T = K_S h/E_T = 0.25$ (black solid lines). The results confirmed that the zigzag model is able to reproduce the results according to Pagano's 2D exact solution (red solid lines).

Figure 7 shows the results for varying interfacial stiffnesses $K_S^1 h/E_T = K_S^2 h/E_T = K_S h/E_T = 0.25$ (black solid lines), 0.75 (black dashed lines) and 5 (black dotted lines). The presence of compliant interfaces induced an increase in absolute values of local displacements and bending stresses, in addition to quite large jumps at the very compliant interfaces. The limit value for the interfacial stiffness for which the 1D solution virtually overlapped to the 2D solution was $K_S h/E_T = 5$, which is half of the value for the two-layer beam. A verification of the accuracy of the zigzag model for the systems in Figures 6 and 7 was presented in [25].

Figure 8 shows the local response for the same beam, but with the two interfaces of different stiffness. The upper interfacial stiffness was assumed to be constant and quite low $K_S^2 h/E_T = 0.25$, whereas that of the lower interface was varied: $K_S^1/K_S^2 = 3$ ($K_S^1 h/E_T = 0.75$, red solid lines), 6 ($K_S^1 h/E_T = 1.5$, blue solid lines) and 10 ($K_S^1 h/E_T = 2.5$, green solid lines). The results obtained in the case of identical interfaces with stiffnesses $K_S^1 h/E_T = K_S^2 h/E_T = 0.75$ (red dotted lines) and 1.5 (blue dotted lines) are also shown.

In order to understand how the interface asymmetry affected the beam response, it is worth comparing the red dotted and solid lines, as an example, that is the results related to interfaces with $K_S^1 h/E_T = K_S^2 h/E_T = 0.75$ (equal interfacial stiffnesses) and those for $K_S^1 h/E_T = 0.75$ and $K_S^2 h/E_T = 0.25$ (different interfacial stiffnesses so that $K_S^1/K_S^2 = 3$). A redistribution of the displacements and stresses in the layers and across the interfaces was evident. The jumps of the longitudinal displacements and bending stresses decreased at the lower stiffer interface, whereas significant increases were experienced by the upper, more compliant interface. Interfacial tractions increased noticeably at the lower interface, whereas they vanished at the upper interface. On the contrary, increasing further the stiffness of the lower interfaces did not affect significantly the local responses.

4. Conclusions

The paper refers to the structural model in [23] which uses a zigzag kinematic approximation and a multiscale approach to analyze layered beams with imperfect interfaces. The model depends on only three displacement variables for any arbitrary number of layers and interfaces and is then more efficient than layer-wise theories where the number of degrees of freedom is proportional to the number of layers. The model is specialized here to mechanical transverse loadings and laminates consisting of layers made of the same material and finds application in the analysis of unidirectional laminated composites, where degradation and delamination of the interfaces are the main failure mechanisms.

A single-variable formulation of the model is derived in order to reduce from three to one the displacement unknowns and the equations governing the problem. The main advantages of this novel formulation are the simplification of the analytical solutions and the numerical implementation of the model, which can use efficient isogeometric schemes. The numerical solution fully avoids the problem of shear-locking.

The application to two- and three-layered beams and the comparison with 2D elasticity solutions highlights the accuracy of the single-variable technique in predicting the important effects of the imperfect interfaces on the local response.

The model reproduces the more or less significant stress and displacement jumps at the interfaces which are controlled by the interfacial stiffnesses. When the stiffnesses of the interfaces are different, noticeable redistributions of both displacements and stresses across the interfaces and in the layers are predicted.

Future extensions of the single-variable model will consider systems with layers made of different materials, which also allow us to describe thick interlayers or transition zones between the adjacent layers, thermal loadings and residual stresses or misfit strains.

Author Contributions: Conceptualization, I.M. and R.M.; methodology and formal analysis, I.M. and R.M.; software, I.M.; validation, I.M.; investigation, I.M. and R.M.; writing, I.M.; project administration and funding acquisition, R.M. All authors have read and agreed to the published version of the manuscript.

Funding: This research was funded by: the U.S. ONR and ONR Global, grant number N62909-21-1-2048; the European Community, NextGenerationEU, code CN00000023, "Sustainable Mobility Center, CNMS" within the National Recovery and Resilience Plan, Mission 4, Component 2, Investment 1.4.

Institutional Review Board Statement: Not applicable.

Informed Consent Statement: Not applicable.

Data Availability Statement: All data that support the findings of this study are included within the article.

Conflicts of Interest: The authors declare no conflict of interest.

Appendix A

In this Appendix all coefficients in the equations governing the model described in Section 2, which are defined in Equations (6), (12), (13), (15) and (17) and used in the paper having chosen a mid-thickness reference surface, are reported.

Appendix A.1. Laminates Consisting of Two Layers Having Equal Thickness

In what follows, posing $K_S^1 = K_S$ and $^{(k)}h = t$ ($k = 1, 2$) so that $h = 2t$, we have:

$$A_{22} = \bar{C}_{22}h, B_{22} = 0, D_{22} = \frac{1}{12}\bar{C}_{22}h^3, \tag{A1}$$

$$C_{22}^{0S} = \frac{\bar{C}_{22}C_{44}t}{K_S}, C_{22}^{1S} = \frac{\bar{C}_{22}C_{44}t^2}{2K_S}, C_{22}^{S2} = \frac{\bar{C}_{22}C_{44}^2t}{K_S^2}, A_{44} = \frac{C_{44}^2}{K_S} + C_{44}k_{44}h, \tag{A2}$$

$$\Omega_4 = -\frac{8K_S(C_{44} + k_{44}K_S h)}{\bar{C}_{22}C_{44}t}, \Omega_3 = -\frac{12K_S(C_{44} + k_{44}K_S h)}{\bar{C}_{22}^2C_{44}t^4}, \Omega_2 = \frac{3(2C_{44} + K_S h)}{\bar{C}_{22}C_{44}t^3}, \tag{A3}$$

$$W_4 = \frac{\bar{C}_{22}^2t^3(2C_{44} + K_S h)}{24K_S(C_{44} + k_{44}K_S h)^2}, W_2 = -\frac{\bar{C}_{22}t^2(3C_{44} + 2K_S h)}{6C_{44}(C_{44} + k_{44}K_S h)}, \tag{A4}$$

$$W_f = -\frac{\bar{C}_{22}(2C_{44} + K_S h)^2}{8C_{44}K_S(C_{44} + k_{44}K_S h)^2},$$

$$V_3 = -\frac{\bar{C}_{22}C_{44}t^2}{12K_S(C_{44} + k_{44}K_S h)}, V_1 = 0, V_f = \frac{2C_{44} + K_S h}{K_S h(C_{44} + k_{44}K_S h)}. \tag{A5}$$

Appendix A.2. Laminates Consisting of Three Layers Having Equal Thickness

In this case, coefficients A_{22} , B_{22} and D_{22} can be written as in Equation (A1), but with $h = 3t$ having posed $^{(k)}h = t$ ($k = 1, \dots, 3$). The other coefficients are:

$$C_{22}^{0S} = \frac{\bar{C}_{22}C_{44}t(K_S^1 + 2K_S^2)}{K_S^1K_S^2}, C_{22}^{1S} = \frac{\bar{C}_{22}C_{44}t^2(K_S^1 + K_S^2)}{K_S^1K_S^2}, \tag{A6}$$

$$C_{22}^{S2} = \frac{\bar{C}_{22}C_{44}^2t[(K_S^1)^2 + 2K_S^1K_S^2 + 2(K_S^2)^2]}{(K_S^1K_S^2)^2}, A_{44} = \frac{C_{44}^2(K_S^1 + K_S^2)}{K_S^1K_S^2} + C_{44}k_{44}h,$$

$$\Omega_4 = -\frac{9K_S^1K_S^2[C_{44}(K_S^1 + K_S^2) + k_{44}K_S^1K_S^2h]}{2\bar{C}_{22}C_{44}t[(K_S^1)^2 - K_S^1K_S^2 + (K_S^2)^2]}, \Omega_3 = -\frac{2K_S^1K_S^2[C_{44}(K_S^1 + K_S^2) + k_{44}K_S^1K_S^2h]}{(\bar{C}_{22})^2C_{44}t^4[(K_S^1)^2 - K_S^1K_S^2 + (K_S^2)^2]}, \tag{A7}$$

$$\Omega_2 = \frac{4C_{44}[(K_S^1)^2 + K_S^1K_S^2 + (K_S^2)^2] + 6K_S^1K_S^2t(K_S^1 + K_S^2)}{3\bar{C}_{22}C_{44}t^3[(K_S^1)^2 - K_S^1K_S^2 + (K_S^2)^2]},$$

$$W_4 = \frac{(\bar{C}_{22})^2t^3[(K_S^1)^2 - K_S^1K_S^2 + (K_S^2)^2]\{2C_{44}[(K_S^1)^2 + K_S^1K_S^2 + (K_S^2)^2] + hK_S^1K_S^2(K_S^1 + K_S^2)\}}{6K_S^1K_S^2(K_S^1 + K_S^2)[C_{44}(K_S^1 + K_S^2) + hk_{44}K_S^1K_S^2]^2}, \tag{A8}$$

$$W_2 = -\frac{\bar{C}_{22}t^2[4C_{44}(K_S^1 + K_S^2) + 3hK_S^1K_S^2]}{4C_{44}[C_{44}(K_S^1 + K_S^2) + hk_{44}K_S^1K_S^2]},$$

$$W_f = -\frac{\bar{C}_{22}\{2C_{44}[(K_S^1)^2 + K_S^1K_S^2 + (K_S^2)^2] + hK_S^1K_S^2(K_S^1 + K_S^2)\}^2}{9C_{44}K_S^1K_S^2(K_S^1 + K_S^2)[C_{44}(K_S^1 + K_S^2) + hk_{44}K_S^1K_S^2]^2},$$

$$V_3 = -\frac{\bar{C}_{22}C_{44}t^2(K_S^1 + 2K_S^2)[(K_S^1)^2 - K_S^1K_S^2 + (K_S^2)^2]}{6K_S^1K_S^2(K_S^1 + K_S^2)[C_{44}(K_S^1 + K_S^2) + hk_{44}K_S^1K_S^2]}, V_1 = 0, \tag{A9}$$

$$V_f = \frac{(K_S^1 + 2K_S^2)\{2C_{44}[(K_S^1)^2 + K_S^1K_S^2 + (K_S^2)^2] + hK_S^1K_S^2(K_S^1 + K_S^2)\}}{3hK_S^1K_S^2(K_S^1 + K_S^2)[C_{44}(K_S^1 + K_S^2) + hk_{44}K_S^1K_S^2]}.$$

Appendix B

In this Appendix the general solution of Equation (11) for the primal variable w_{0b} is provided for laminates satisfying the condition $\Omega_4 < 0$.

In this case, the roots of the characteristic equation, associated with the homogeneous differential Equation (11) with $f_3 = 0$, are $= \pm\sqrt{-\Omega_4}$ and $= 0$ having multiplicity 4. The general solution of Equation (11) is then given in the form

$$w_{0b} = c_1 \cosh(\lambda x_2) + c_2 \sinh(\lambda x_2) + c_3 \frac{x_2^3}{6} + c_4 \frac{x_2^2}{2} + c_5 x_2 + c_6 + \bar{w}_{0b}, \quad (\text{A10})$$

where $\lambda = \sqrt{-\Omega_4}$ and \bar{w}_{0b} is a particular solution of Equation (11) depending on the distributed transverse load. For a sinusoidal transverse load $f_3(x_2) = q_0 \sin(\pi x_2/L)$, then

$$\bar{w}_{0b}(x_2) = q_0 L^4 \sin(\pi x_2/L) (\pi^2 \Omega_2 - L^2 \Omega_3) / [\pi^4 (\pi^2 - L^2 \Omega_4)]. \quad (\text{A11})$$

For a uniform transverse load $f_3(x_2) = q_0$, then

$$\bar{w}_{0b}(x_2) = q_0 x_2^4 \Omega_3 / (24 \Omega_4). \quad (\text{A12})$$

References

- Begley, M.R.; Hutchinson, J.W. *The Mechanics and Reliability of Films, Multilayers and Coatings*; Cambridge University Press: Cambridge, UK, 2017.
- Berggreen, C.; Saseendrana, V.; Carlsson, L.A. A modified DCB-UBM test method for interfacial fracture toughness characterization of sandwich composites. *Eng. Fract. Mech.* **2018**, *203*, 208–223. [\[CrossRef\]](#)
- Massabò, R. Effective modeling of interlaminar damage in multilayered composite structures using zigzag kinematic approximations. In *Handbook of Damage Mechanics*; Voyiadis, G.Z., Ed.; Springer: New York, NY, USA, 2020; pp. 1–34.
- Abrate, S.; Di Sciuva, M. Multilayer models for composite and sandwich structures. In *Comprehensive Composite Materials II*; Zweben, C.H., Beaumont, P.W.R., Eds.; Elsevier: Amsterdam, The Netherlands, 2018; pp. 399–425.
- Monetto, I. The effects of an interlayer debond on the flexural behavior of three-layer beams. *Coatings* **2019**, *9*, 258. [\[CrossRef\]](#)
- Di Sciuva, M. Bending, vibration and buckling of simply supported thick multilayered orthotropic plates: An evaluation of a new displacement model. *J. Sound Vib.* **1986**, *105*, 425–442. [\[CrossRef\]](#)
- Di Sciuva, M. An improved shear-deformation theory for moderately thick multilayered anisotropic shells and plates. *J. Appl. Mech.* **1987**, *54*, 589–596. [\[CrossRef\]](#)
- Averill, R.C. Static and dynamic response of moderately thick laminated beams with damage. *Compos Eng.* **1994**, *4*, 381–395. [\[CrossRef\]](#)
- Carrera, E. Historical review of zig-zag theories for multilayered plates and shells. *Appl. Mech. Rev.* **2003**, *56*, 287–308. [\[CrossRef\]](#)
- Tessler, A.; Di Sciuva, M.; Gherlone, M. A refined zigzag beam theory for composite and sandwich beams. *J. Compos. Mater.* **2009**, *43*, 1051–1081. [\[CrossRef\]](#)
- Iurlaro, L.; Gherlone, M.; Di Sciuva, M.; Tessler, A. Refined zigzag theory for laminated composite and sandwich plates derived from Reissner's mixed variational theorem. *Compos. Struct.* **2015**, *133*, 809–817. [\[CrossRef\]](#)
- Tessler, A. Refined zigzag theory for homogeneous, laminated composite, and sandwich beams derived from Reissner's mixed variational principle. *Meccanica* **2015**, *50*, 2621–2648. [\[CrossRef\]](#)
- Groh, R.M.J.; Tessler, A. Computationally efficient beam elements for accurate stresses in sandwich laminates and laminated composites with delaminations. *Comput. Methods Appl. Mech. Eng.* **2017**, *320*, 369–395. [\[CrossRef\]](#)
- Antes, H. Fundamental solution and integral equations for Timoshenko beams. *Comput. Struct.* **2003**, *81*, 383–396. [\[CrossRef\]](#)
- Falsone, G.; Settineri, D. An Euler–Bernoulli-like finite element method for Timoshenko beams. *Mech. Res. Commun.* **2011**, *38*, 12–16. [\[CrossRef\]](#)
- Reddy, J.N. *An Introduction to the Finite Element Method*; McGraw-Hill: New York, NY, USA, 1993.
- Marino, E. Locking-free isogeometric collocation formulation for three-dimensional geometrically exact shear-deformable beams with arbitrary initial curvature. *Comput. Methods Appl. Mech. Eng.* **2017**, *324*, 546–572. [\[CrossRef\]](#)
- Kiendl, J.; Auricchio, F.; Hughes, T.J.R.; Reali, A. Single-variable formulations and isogeometric discretizations for shear deformable beams. *Comput. Methods Appl. Mech. Eng.* **2015**, *284*, 988–1004. [\[CrossRef\]](#)
- Kiendl, J.; Auricchio, F.; Reali, A. A displacement-free formulation for the Timoshenko beam problem and a corresponding isogeometric collocation approach. *Meccanica* **2018**, *53*, 1403–1413. [\[CrossRef\]](#)
- Monetto, I.; Massabò, R. A single-variable approach for layered beams with imperfect interfaces. In Proceedings of the XXV Conference AIMETA, Palermo, Italy, 4–8 September 2022. *in press*.
- Massabò, R.; Monetto, I. Modeling imperfect interfaces in layered beams through multi- and single-variable zigzag kinematics. In Proceedings of the 8th European Congress on Computational Methods in Applied Sciences and Engineering—ECCOMAS Congress 2022, Oslo, Norway, 5–9 June 2022. *in press*.

22. Auricchio, F.; da Veiga, L.B.; Hughes, T.J.R.; Reali, A.; Sangalli, G. Isogeometric collocation methods. *Math. Mod. Meth. Appl. Sci.* **2010**, *20*, 2075–2107. [[CrossRef](#)]
23. Pelassa, M.; Massabò, R. Explicit solutions for multi-layered wide plates and beams with perfect and imperfect bonding and delaminations under thermo-mechanical loading. *Meccanica* **2015**, *50*, 2497–2524. [[CrossRef](#)]
24. Massabò, R.; Campi, F. Assessment and correction of theories for multilayered plates with imperfect interfaces. *Meccanica* **2015**, *50*, 1045–1071. [[CrossRef](#)]
25. Massabò, R.; Campi, F. An efficient approach for multilayered beams and wide plates with imperfect interfaces and delaminations. *Compos. Struct.* **2014**, *116*, 311–324. [[CrossRef](#)]
26. Massabò, R. Influence of boundary conditions on the response of multilayered plates with cohesive interfaces and delaminations using a homogenized approach. *Frat. Integrità Strutt.* **2014**, *8*, 230–240.
27. Massabò, R.; Darban, H. Mode II dominant fracture of layered composite beams and wide-plates: A homogenized structural approach. *Eng. Fract. Mech.* **2019**, *213*, 280–301. [[CrossRef](#)]
28. Massabò, R.; Monetto, I. Local zigzag effects and brittle delamination fracture of n-layered beams using a structural theory with three displacement variables. *Frat. Integrità Strutt.* **2020**, *51*, 275–287. [[CrossRef](#)]
29. Sburlati, R.; Monetto, I. Effect of an inhomogeneous interphase zone on the bulk modulus of a particulate composite containing spherical inclusions. *Compos. Part B Eng.* **2016**, *97*, 309–316. [[CrossRef](#)]
30. Darban, H.; Massabò, R. A homogenized structural model for shear deformable composites with compliant interlayers. *Multiscale Multidiscip. Model. Exp. Des.* **2018**, *1*, 269–290. [[CrossRef](#)]
31. Pagano, N.J. Exact solutions for composite laminates in cylindrical bending. *J. Compos. Mater.* **1969**, *3*, 398–411. [[CrossRef](#)]
32. Darban, H.; Massabò, R. Thermo-elastic solutions for wide plates and beams with interfacial imperfection through the transfer matrix method. *Meccanica* **2018**, *53*, 553–571. [[CrossRef](#)]

Disclaimer/Publisher’s Note: The statements, opinions and data contained in all publications are solely those of the individual author(s) and contributor(s) and not of MDPI and/or the editor(s). MDPI and/or the editor(s) disclaim responsibility for any injury to people or property resulting from any ideas, methods, instructions or products referred to in the content.